An analytical solution to the dynamic behavior of heat exchanger networks

Jiaxing Chen, Guomin Cui *, Yuan Xiao

School of Energy and Power Engineering, University of Shanghai for Science and Technology, Shanghai 200093, PR China

ARTICLE INFO

ABSTRACT

A novel method combined signal flow graph of a single heat exchanger with the transfer function of streams is developed for the dynamic behaviors of heat exchanger networks problems, which are determinate factors of the process control and operation optimization in the processing industries. The transfer functions between any two nodes of heat exchanger networks including the inlet and the outlet are obtained based on the signal flow graph of the networks by block-diagram reduction, Mason's rule and the seeking-up method. The developed method is solved by a numerical inverse Laplace transform and the analytical solution to the dynamic behavior of heat exchanger networks is presented in the time domain. The numerical results demonstrate that the presented method is more efficient and more accurate for the dynamic behaviors of heat exchanger networks problems.

© 2018 Published by Elsevier Ltd.

1. Introduction

The dynamic behavior of heat exchanger networks (HEN) has been taken into consideration because its dynamic response of outlet parameters to the disturbances of inlet parameters is important for the process controllability and operation optimization of the HEN problems [1–3]. Nowadays, substantial numerical and experimental investigations have been carried out for the dynamic behavior of HEN, even including a single heat exchanger due to its wide applications [4–9]. For a single heat exchanger, many dynamic mathematics models [10–16] have been presented by scholars. The results showed that the transient temperature responses of streams can be obtained using analytic methods [17,18] or numerical methods [19,20].

For the HEN problems, the excessive simplifications of the dynamic mathematics model lead to low quality of dynamic simulations, whereas more consideration of the actual conditions in HEN would make the model complicated and increase computational cost. Therefore, the dynamic mathematics model is far from sufficient to apply to the dynamic characteristics of HEN with consideration into more factors [21]. Above all, achieving an efficient and high-accurate solution for the dynamic behavior of the HEN problems is more important than proposing a dynamic mathematics model which can be solved based on the modeling of single heat exchanger.

During the past few decades, many effective numerical methods benefiting from the progress of the dynamic modeling of HEN have been presented to investigate the dynamic behavior of HEN [22–29]. Mathisen et al. [22] proposed a dynamic model of relatively simple HEN taking the structure, pipe residence time, model order of bypasses and the connecting pipes into consideration. The dynamic model based on the lumped model for a single heat exchanger was solved using the state-space method for the dynamic behavior of HEN and was implemented in Simulink. It's shown that the presented dynamic model can be not for more complicated HEN owing to modeling complexity, computational speed, and numerical stability. Several dynamic models for HEN have been developed for the dynamic behavior of HEN problems in different practical requirements [23–26]. Boyaci et al. [27] used a distributed-parameter model consisting of multi-tube, single-pass heat exchangers to construct a dynamic model of the HEN and investigated numerically the transient behavior of the HEN. Baldea et al. [28] presented a procedure deriving reduced-order, non-stiff models, which was focused on the dynamics and control of HEN consisting of a reactor connected with an external heat exchanger through a large material recycle stream that acts as an energy carrier. Guha and Ghaudhuri [29] developed a mathematical model to describe the transient heat exchange between the process streams of HEN and solved the developed model by a finite difference numerical scheme and solution algorithm.

Although numerical methods can almost deal properly with the dynamic behavior of all types of HEN problems, the methods are invalid for real-time control. Moreover, higher computational

---

* Corresponding author.
  E-mail address: cgm@usst.edu.cn (G. Cui).

Nomenclature

A	area of heat exchanger, m^2	*Subscripts*	
C_p	specific heat of the stream, kJ/(kg K)	c	cold stream
G	mass flow rate, kg/s	h	hot streams
K	gain	i	inlet
T	time constant	o	outlet
$U(s)$	inlet parameter of transfer function	q	heat
v	velocity of stream, m/s	t	temperature
$W(s)$	operator transmittance	w	metal wall of heat exchanger
$Y(s)$	outlet parameter of transfer function		
h	heat transfer coefficient, W/(m^2 K)		
τ	delay time, s		

---

efforts and costs are required when the methods are implemented for more complicated and larger-scale HEN. Nowadays, analytical solution of HEN has drawn attentions from many researchers due to its high efficiency for dynamic behavior of HEN.

In present study, a novel method based on signal flow graphs is established to obtain an analytical solution for the dynamic behavior of HEN. First, a single heat exchanger is treated as a 4×4 Multiple-Input Multiple-Output (MIMO) system, and the signal flow graph of the HEN is established according to the transitive relation among streams. Second, three methods (block-diagram reduction, Mason's rule and seeking up) are used to obtain the transfer function from the inlet to outlet nodes or between any two random nodes. Finally, according to a numerical inverse Laplace transform, an analytical solution for the dynamic behavior of HEN is presented in the time domain.

2. Approaches

2.1. Transfer functions and signal flow graph for a single heat exchanger

For the HEN system, the outlet temperature response of a single heat exchanger can be approximated to transfer function of a first-order or second-order inertial element. In present study, the first-order model with time delay used to the simplification for the transient profile of heat exchangers [30,31] is employed to describe the dynamic behavior of the single heat exchanger. Therefore, Therefore, the ratio of output temperature $Y(s)$ to input disturbance $U(s)$ in the Laplace domain can be given as [32],

$$W(s) = \frac{Y(s)}{U(s)} = \frac{K}{Ts+1} e^{-\tau s} \qquad (1)$$

where K, T and τ are shown in the Appendix A. The three dynamic parameters are obtained by the logarithmic mean temperature difference for higher static accuracy. Detailed derivation process of K, T and τ can be seen in the Sections 2-4 of previous research [33].

With similar to other heat-exchanger models in which the absence of fluid phase-change [22,34,35], the simplifying assumptions are following: (1) the heat-exchanging fluids are fully mixed and their temperatures are constant; (2) both cold and hot fluids are incompressible and their pressure drops are negligibly small, it is often appropriate to assume that delay effect only acts on the stream with inlet temperature disturbance, and time constant is identical for temperature and flow-rate disturbances; (3) thermal-physical parameters of both cold and hot fluids and tube-wall materials are constant; (4) heat conduction between units can be neglected; (5) heat accumulation in the shell wall material can be neglected; (6) the values of heat transfer coefficients determined for steady state conditions remain unchanged

in transient states; (7) heat losses to the environment are negligibly small.

For a single heat exchanger shown in Fig. 1(a), there are four potential disturbances including flow disturbances and temperature disturbances of the cold and hot inlet streams. Therefore, the outlet temperature responses of cold and hot streams in single heat exchanger can be expressed as follows,

$$\Delta t_{co}(s) = W_{ctc}(s)\Delta t_{ci}(s) + W_{cth}(s)\Delta t_{hi}(s) + W_{cGc}(s)\Delta G_{ci}(s)$$
$$+ W_{cGh}(s)\Delta G_{hi}(s) \qquad (2)$$

$$\Delta t_{ho}(s) = W_{hth}(s)\Delta t_{hi}(s) + W_{htc}(s)\Delta t_{ci}(s) + W_{hGc}(s)\Delta G_{ci}(s)$$
$$+ W_{hGh}(s)\Delta G_{hi}(s) \qquad (3)$$

In addition to the outlet temperature responses, which are expressed as functions of all inlet disturbances, the responses of the outlet flow rate are also treated as functions of the inlet
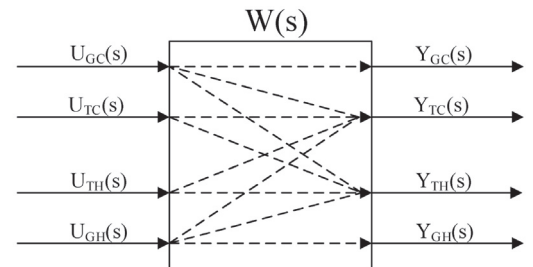
(a) Transfer function of heat exchanger
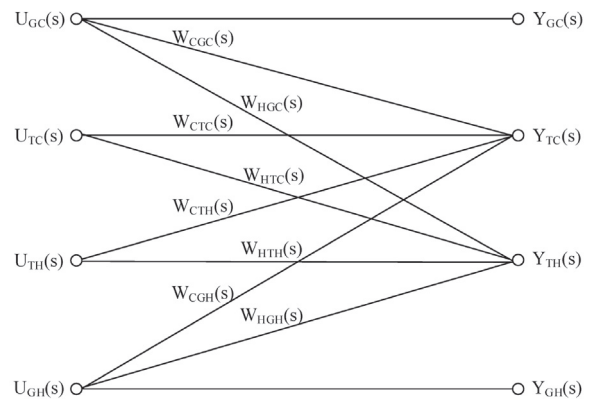
(b) Signal flow graph of heat exchanger

Fig. 1. Transfer function and signal flow graph of heat exchanger.

(a) 2×2 HEN

(b) Signal flow graph of the network
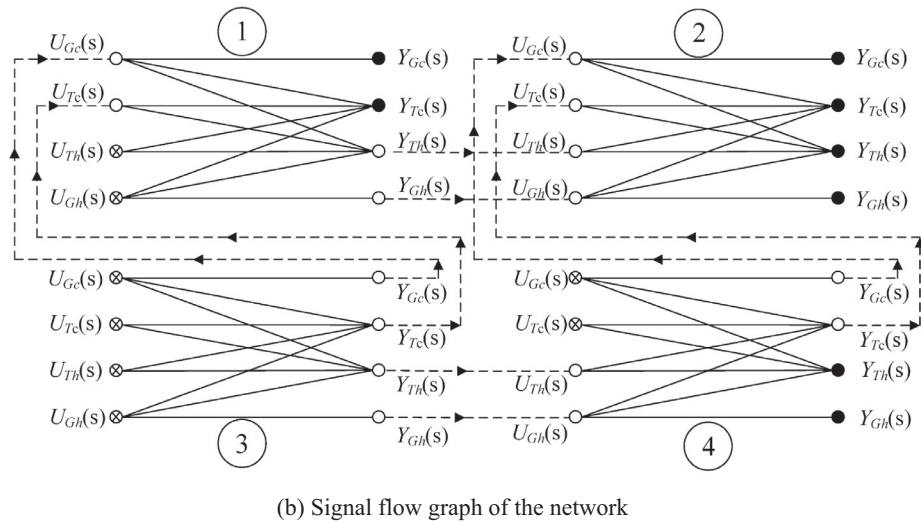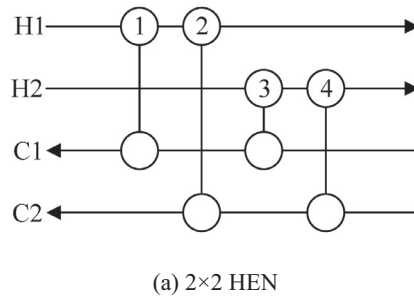
Fig. 2. The structure and signal flow graph of the HEN.

parameters of themselves with transfer function $W(s) = 1$. Consequently, the output responses of a heat exchanger correspond to a 4×4 MIMO system expressed by Eqs. (2) and (3). Meanwhile, the signal flow graph of a single heat exchanger is obtained as Fig. 1(b).

2.2. Signal flow graph of heat exchanger networks

Including all transfer relationships of temperature and flow rate, an attempt is made to turn the dynamic input-output relation of HEN into signal flow graph like that of a single heat exchanger in Section 2.1.

In HEN, the streams flows through each heat exchanger, successively. The parameters of the inlet stream of the next exchanger are identical with the outlet parameters of the previous exchanger, that is, the change of the outlet signal of the previous exchanger is assigned to the inlet signal of the next exchanger. A signal flow graph of HEN can be constructed based on the transfer relationship. Taking a 2×2 HEN example, which is shown in the form of the stage-wise superstructure as Fig. 2(a) by Yee and Grossmann [36], the dynamic transfer relationship is depicted by the signal flow graph as shown in Fig. 2(b).

The signal flow graph is an analytical tool to model discrete event systems [37]. For the HEN problem, it offers a diagram of causal relationships among a number of the components in the HEN system. For HEN (as shown in Fig. 2), temperatures and flow rates in the inlet and outlet nodes of each single heat exchanger
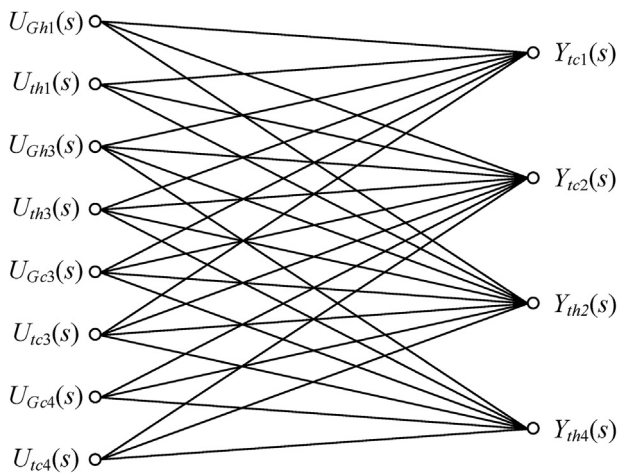
Fig. 3. Signal flow graph after simplified.

Table 1
Data of streams and heat exchangers.

HE	Stream	A/m^2	$(GCp)/kW/K$	$h/kW/(m^2 \, K)$	T/s	τ/s
HE1	H4	42.54	27.26	1.0	5.69	4.44
	C3		14.53		5.69	3.92
HE2	H2	25.98	21.04	1.0	16.50	8.33
	C3		14.53		16.50	7.93
HE3	H1	37.56	41.45	1.2	12.61	6.67
	C3		14.53		12.61	7.84
HE4	H4	37.50	27.26	1.0	6.21	5.55
	C2		15.40		6.21	3.62
HE5	H1	52.64	41.45	0.8	5.71	3.33
	C2		15.40		5.71	3.5
HE6	H3	30.23	38.82	1.5	4.55	4.44
	C2		15.40		4.55	3.58
HE7	H4	15.62	27.26	0.6	3.94	2.66
	C1		16.07		3.94	3.17
HE8	H1	55.03	41.45	0.5	8.37	5.07
	C4		14.11		8.37	4.67
HE9	H3	85.18	38.82	1.2	3.97	3.06
	C5		13.78		3.97	3.33

are treated as variables, which are called 'signals' in the signal flow graph. The outlet parameters of HEN and the parameters in any node can be taken as terminal outputs. This way would greatly improve the analysis depth and extent of HEN.

In Fig. 2(b), it can be seen that there are 8 nodes (4 input nodes U and 4 output nodes Y) for the signal flow graph of each heat exchanger. The x-shape circle in the figure represents the source node of the input signal for HEN with only signal output. It indicates the change in the parameters of the initial flow input. While the solid circle represents the joint node of the output signal for network with only signal input. It indicates the change in the parameters of the final flow output. And the hollow circle represents the intermediate node which transfers the intermediate signal for HEN transmission, known as the mixed node. Thus, there are both signal input and signal output in the mixed node. The expression on the solid line is the transfer function while the dotted line plays the role of connection without any change in signal. Besides, the mathematical operator next to the branch connecting

two nodes is the transfer function. The end signal of the branch is equal to the starting signal multiplied by the transfer function of the branch.

2.3. Solving the dynamic behavior of heat exchanger networks

With the signal flow graph represented above, the Laplace domain outputs of the whole network (including both outlet nodes and intermediate nodes) can be obtained. According to the topological property of the signal flow graph, three methods are used to determine the transfer functions in present study.

2.3.1. Block-diagram reduction

According to the simplification rule (including addition, multiplication, distribution, and factoring) of signal flow graph, the mixed nodes with input signal and output signal are eliminated to reduce the number of branches and nodes in the signal flow graph, leaving only the source nodes and the joint nodes. So that the transfer function between the source node and the sink node is obtained. According to the transfer function, the dynamic behaviors of HEN are presented. Due to the reduction of the nodes, the mothed is called Block-diagram reduction.

According to the Block-diagram reduction, a simplified signal flow graph of Fig. 2(b) is shown in Fig. 3. It can be seen that there are only source nodes and joint nodes. After simplification, there are still only output branches on the source nodes and input branches is on the joint nodes. So every node in the figure represents an input or output signal of the heat exchange system.

In the above calculation procedure, the outputs of the intermediate nodes can also be achieved. However, this method can only be applied to networks without loops. For the networks with loops, the signal flow diagram could not be simplified to include only the source node and the sink node due to its feedback loop. Therefore, other methods should be chosen and proposed for the dynamic studies of networks with loops, such as the following method using Mason's rule.
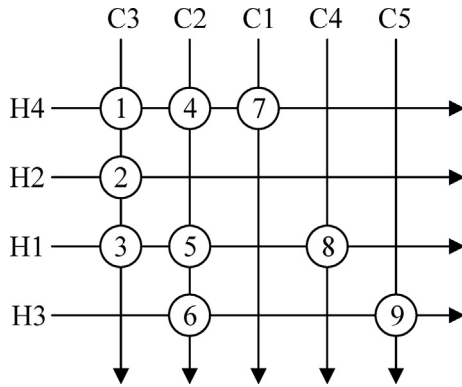
Fig. 4. Structure of the HEN.
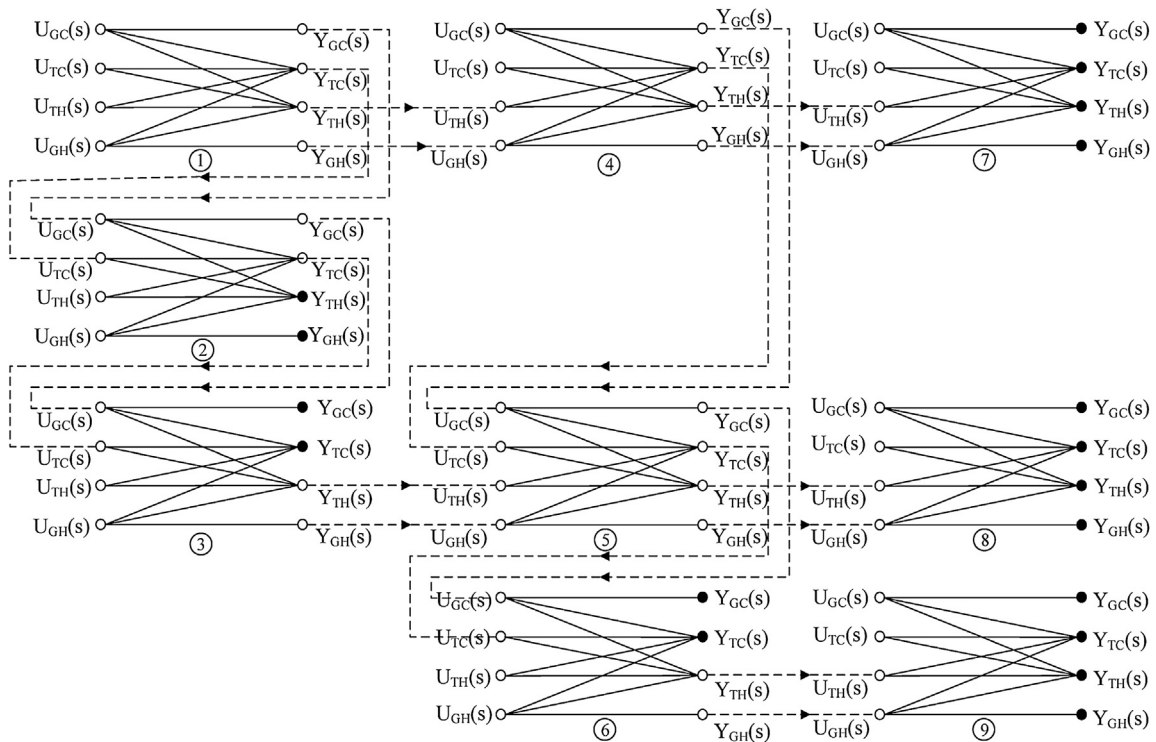
Fig. 5. Signal flow graph of the HEN.

2.3.2. Using Mason's rule

A signal flow graph can also be implemented using Mason's rule [38]. This rule correlates the graph to the algebra of the simultaneous equations. Accordingly, the input-output transfer function can be directly given by:

$$W(s) = \frac{Y(s)}{U(s)} = \frac{1}{\Delta} \sum_{k=1}^{n} P_k \Delta_k \qquad (4)$$

$$\Delta = 1 - \sum L_a + \sum L_b L_c - \sum L_d L_e L_f + \cdots \qquad (5)$$

where Δ is the system determinant, Δ_k is the value of Δ for that part of the graph not touching the kth forward path, P_k is gain of the kth forward path. $\sum L_a$ is all individual loop gains and $\sum L_b L_c$ and $\sum L_d L_e L_f$ denote the gain products of all possible two loops and three loops that do not touch, respectively.

To obtain the transfer functions of HEN, the sub-transfer functions of the specified joint node to each source node is firstly given using Mason's rule and then the transfer function of the specified joint node is the sum of these sub-transfer functions. Taking outlet node Y_{tc1} as the specified node, the sub-transfer functions of Y_{tc1} to U_{Gc3}, U_{th1}, U_{Gh1}, U_{tc3}, U_{th3} and U_{Gh3} are as follows by Mason's rule:

$$Y_{tc1}(s)/U_{Gc3}(s) = W_{cGc1}(s) + W_{cGc3}(s) \times W_{ctc1}(s) \qquad (6)$$

$$Y_{tc1}(s)/U_{th1}(s) = W_{cth1}(s) \qquad (7)$$

$$Y_{tc1}(s)/U_{Gh1}(s) = W_{cth1}(s) \qquad (8)$$

$$Y_{tc1}(s)/U_{tc3}(s) = W_{ctc3}(s) \times W_{ctc1}(s) \qquad (9)$$

$$Y_{tc1}(s)/U_{th3}(s) = W_{cth3}(s) \times W_{ctc1}(s) \qquad (10)$$

$$Y_{tc1}(s)/U_{Gh3}(s) = W_{cth3}(s) \times W_{ctc1}(s) \qquad (11)$$

These transfer functions have simple forms because there are only forward paths between two nodes with $\Delta = 1$. Summing the individual output yields, the total output $Y_{tc1}(s)$ is:

$$\begin{aligned} Y_{tc1}(s) = &[W_{cGc1}(s) + W_{cGc3}(s) \times W_{ctc1}(s)] \times U_{Gc3}(s) + W_{cth1}(s) \\ &\times U_{th1}(s) + W_{cth1}(s) \times U_{Gh1}(s) + W_{ctc3}(s) \times W_{ctc1}(s) \\ &\times U_{tc3}(s) + W_{cth3}(s) \times W_{ctc1}(s) \times U_{th3}(s) + W_{cth3}(s) \\ &\times W_{ctc1}(s) \times U_{Gh3}(s) \end{aligned}$$
$$(12)$$

The output given in Mason's rule has the same form and value as that in block-diagram reduction, but the advantage of Mason's rule is the systematic and algorithmic characteristics, especially for complicated block diagrams with loops.

2.3.3. Seeking up

Based on the structure of HEN, the seeking up method is used to obtain the output of the signal flow graph directly without removing intermediate nodes. The output of the graph is described as follows:

(1) Start from the specified joint node, and then search the preceding nodes on the input branches. Then, the specified joint node can be expressed using these preceding nodes. Taking the outlet temperature of the 4th heat exchanger in Fig. 2 (b) as an example, its preceding nodes are $U_{Gc4}(s)$, $U_{tc4}(s)$, $U_{th4}(s)$ and $U_{Gh4}(s)$, so $Y_{th4}(s)$ can be expressed as:

$$\begin{aligned} Y_{th4}(s) = &W_{hGc4}(s) \times U_{Gc4}(s) + W_{htc4}(s) \times U_{tc4}(s) \\ &+ W_{hth4}(s) \times U_{th4}(s) + W_{hth4}(s) \times U_{Gh4} \end{aligned} \qquad (13)$$

(2) Finishing the above one-step operation, it is necessary to determine the properties of the preceding nodes. If the preceding node is a source node, then a sub-output of this path is gained. Otherwise, the preceding nodes of the current node should be searched as the rule step (1). For this example, in the current preceding nodes $U_{Gc4}(s)$, $U_{tc4}(s)$, $U_{th4}(s)$ and $U_{Gh4}(s)$, two nodes $U_{Gc4}(s)$ and $U_{tc4}(s)$ are source nodes, and the sub-output can be given by

$$Y_{Gc4}(s)/U_{Gc4}(s) = W_{hGc4} \qquad (14)$$

$$Y_{th4}(s)/U_{tc4}(s) = W_{htc4}(s) \qquad (15)$$

(3) Because $U_{th4}(s)$ and $U_{Gh4}(s)$ are intermediate nodes, the preceding nodes of $U_{th4}(s)$ and $U_{Gh4}(s)$ should be searched as the rule step 1) until all nodes are start nodes.

$$\begin{aligned} U_{th4}(s) = Y_{th3}(s) = &W_{hGc3}(s) \times U_{Gc3}(s) + W_{htc3}(s) \times U_{tc3}(s) \\ &+ W_{hth3}(s) \times U_{th3}(s) + W_{hth3}(s) \times U_{Gh3} \end{aligned} \qquad (16)$$

$$U_{Gh4}(s) = U_{Gh3}(s) \qquad (17)$$

(4) When all nodes $U_{Gc3}(s)$, $U_{tc3}(s)$, $U_{th3}(s)$ and $U_{Gh3}(s)$ are all start nodes, searching is terminated. And then summing all sub-outputs, the total output is given in the Appendix C.

The above three methods can help solve any specified output in a signal-flow graph of HEN, and can obtain the temperature response
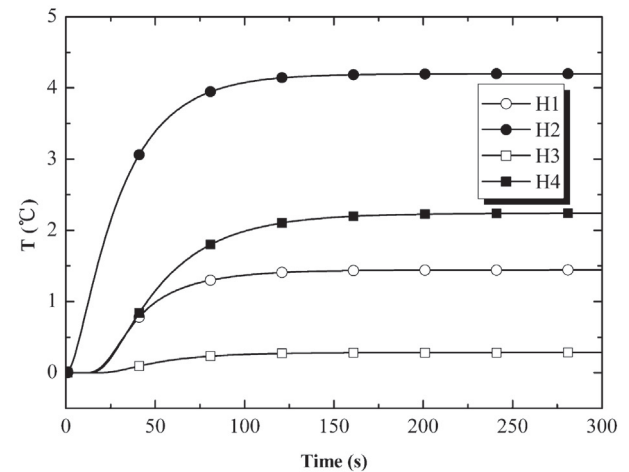
(a) Outlet temperature responses of hot fluids
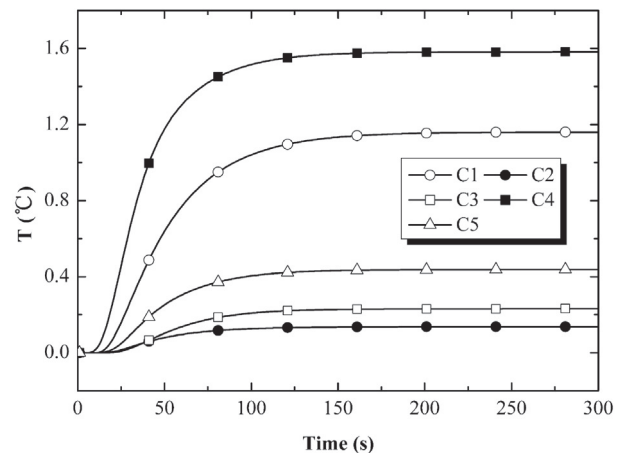
(b) Outlet temperature responses of cold fluids

Fig. 6. Case 1 of transient process under single disturbance.

(in the complex domain) of any specified node. The first method (block-diagram reduction) is more suitable for HEN without loops at the advantage of its low computational requirement. However, for relatively complicated systems, such as those with loops, the second method (Mason's rule) is more useful to solve them manually due to its systematic and algorithmic characteristics, as stated above. The third method (seeking up) is restricted to networks without loops. And it is a problem-dependent method which depends on the experience of the investigators. The third method will result in higher efficiency and real-time debugging in the solution process for some special conditions in HEN, such as the HEN without loops and HEN simulation of higher efficiency requirements.

Once the Laplace domain output of a signal-flow graph (which represents a corresponding HEN) is solved, the time-domain response can be gained by an inverse Laplace transform. Furthermore, an analytical solution to the dynamic behavior of HEN can be obtained. For relatively simple systems, it is easier to perform the inverse Laplace transform manually. However, for more complex systems, a numerical inverse Laplace transform should be employed, which can be achieved using computer-aided software, such as MATLAB.

3. Results and discussion

To validate the proposed method, a 4×5 test HEN case corresponding to Chen et al. [39] is examined using the computer data

listed in Table 1. The structure of the HEN is shown in Fig. 4. According to the transform method, it transfers into the signal-flow graph of the HEN as shown in Fig. 5. Meanwhile, the Laplace domain outputs of the outlet temperatures are obtained by any of the three Laplace transform methods in Section 2.3. And then substituting the disturbances into the Laplace outputs, the time-domain output responses of the HEN are obtained using the inverse Laplace transform. The details of the Laplace transforms and the inverse Laplace transforms are listed in the Appendix D and the Appendix E, respectively.

3.1. Transient process under a single disturbance

For the first case of a single disturbance, from 433 K to 443 K with the inlet temperature disturbance of 10 K for hot stream H4 is given at some time. The according Laplace transform of this disturbance is 10/s in the complex field. Fig. 6(a) and (b) shows the transient responses of the outlet temperature of the hot and cold streams. It can be observed that the time delays of the streams C3, τ_{HE3}, τ_{HE5} and τ_{HE8} become increasingly longer, that is, the time delay effect is magnified step-by-step along the signal traveling direction.

For the second case of a single disturbance, the mass flow rate disturbance from 3.5 kg/s to 3.6 kg/s with the percentage of 2.86% for cold stream C3 is given at some time. The transient
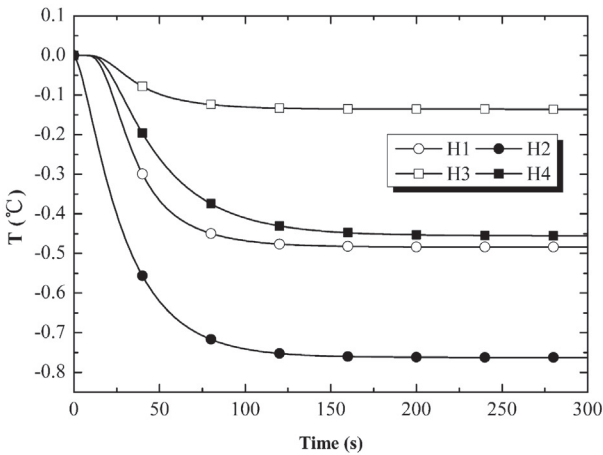
(a) Outlet temperature responses of hot fluids

(a) Outlet temperature responses of hot fluids
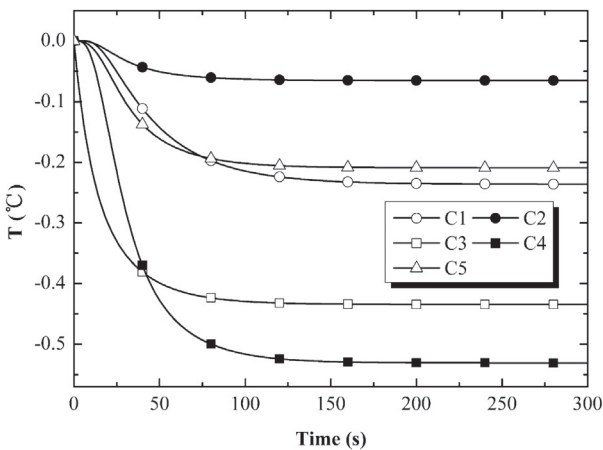
(b) Outlet temperature responses of cold fluids

Fig. 7. Case 2 of transient process under single disturbance.
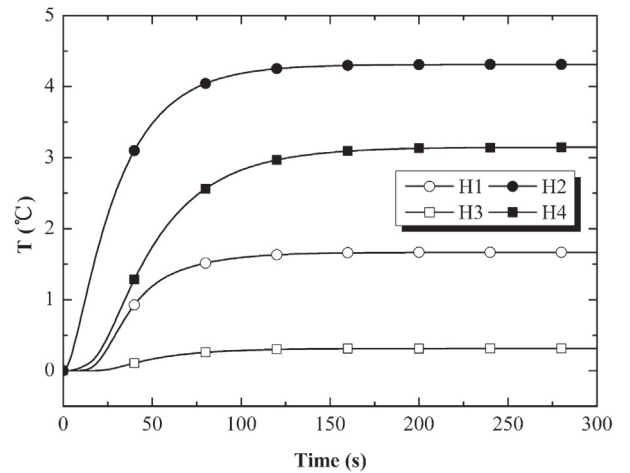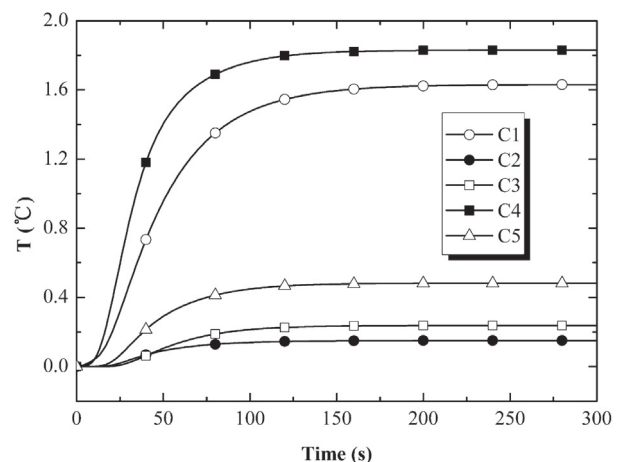
(b) Outlet temperature responses of cold fluids

Fig. 8. Case 1 of transient process under multi disturbances.

responses of the outlet temperature of the hot and cold streams are shown in Fig. 7. It can be seen that there is little time delay for the flow rate changes of incompressible fluids. However, most of the outlet temperature responses present the characteristics of multi-capacity objects due to the inertial effects of heat transfer through all segments.

3.2. Transient process under multi-disturbances

For the first case of multi-disturbance, the inlet temperature disturbance of 10 K (from 433 K to 443 K) and the mass flow rate disturbance from 4.0 kg/s to 4.06 kg/s with the percentage of 1.5% for hot stream H4 are given at some time. The transient responses of the outlet temperature under temperature and flow rate disturbances are shown in Fig. 8. It demonstrates that the tendencies of the temperature responses under temperature and flow rate disturbances in Fig. 8 are basically same with that under the single disturbance of temperature shown in Fig. 6. Compared with Figs. 6 and 7, the time delay under temperature and flow rate disturbances of Fig. 8 are basically same with that under the single disturbance of temperature shown in Fig. 6. Therefore, the time delay of incompressible fluid mainly comes from the temperature disturbance instead of the flow rate disturbance. The results are in good agreement with that of Cui et al. [33].

For the second case of multi-disturbance, the inlet temperature disturbance of -5K (from 358 K to 353 K) for the cold stream C3

and the mass flow rate disturbance from 4.0 kg/s to 4.06 kg/s with the percentage of 1.5% for hot stream H4 are given at same time. The transient responses of the outlet temperature under temperature and flow rate disturbances are shown in Fig. 9. It can be seen from Fig. 9(a) that the outlet temperature of hot stream H4 to increase during the initial period of the transitions because the flow rate disturbance acts ahead of the temperature disturbance. And then, the outlet temperature of hot stream H4 decreases after the time delay of the temperature disturbance. Finally, the outlet temperature becomes steady and is lower than that before the disturbance. The signal-flow graph method clearly provides the priority of the temperature disturbance to the flow rate disturbance.

For the third case of multi-disturbance, the inlet temperature disturbance of 10 K (from 433 K to 443 K) and the mass flow rate disturbance from 4.0 kg/s to 4.06 kg/s with the percentage of 1.5% for the hot stream H4 are given while the cold stream C3 is implemented the inlet temperature disturbance of −5 K (form 358 K to 353 K) and the mass flow rate disturbance from 3.5 kg/s to 3.6 kg/s with the percentage of 2.85%. The transient responses of the outlet temperature under temperature and flow rate disturbances are shown in Fig. 10. It can be seen that the outlet temperature of the cold stream C3 under multi- disturbances increases by about 0.4 K after it reaches steady state. It is in good agreement with the results obtained by the steady simulation method of HEN in the literature [39]. Therefore, the developed method can
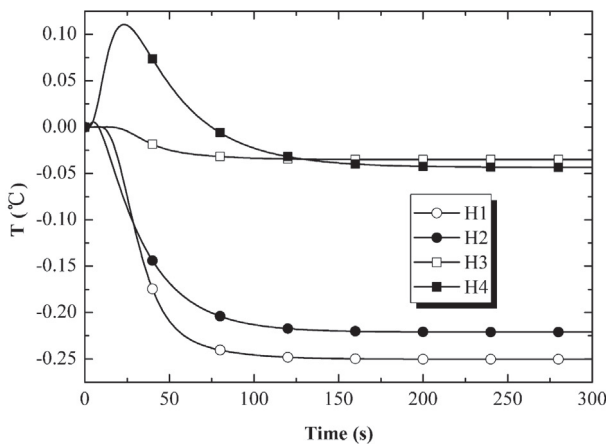
(a) Outlet temperature responses of hot fluids
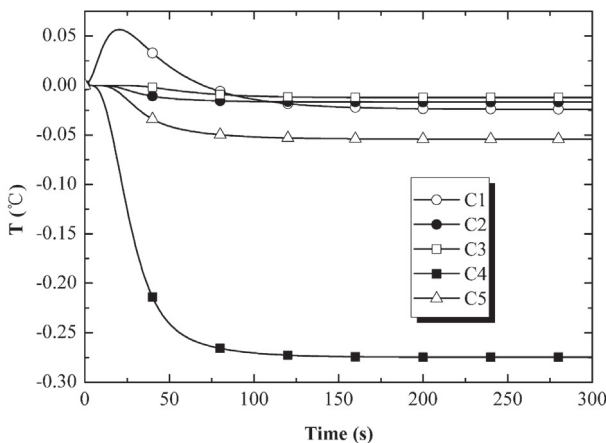
(b) Outlet temperature responses of cold fluids

Fig. 9. Case 2 of transient process under multi disturbances.
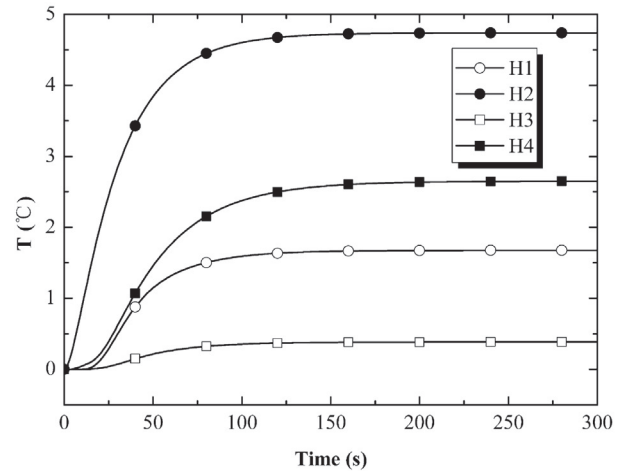
(a) Outlet temperature responses of hot fluids
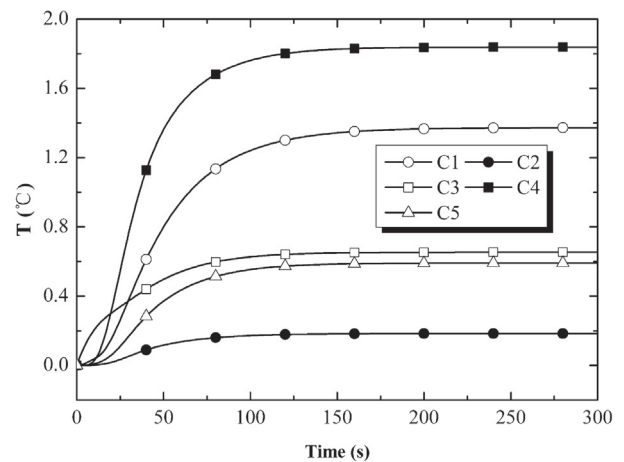
(b) Outlet temperature responses of cold fluids

Fig. 10. Case 3 of transient process under multi disturbances.
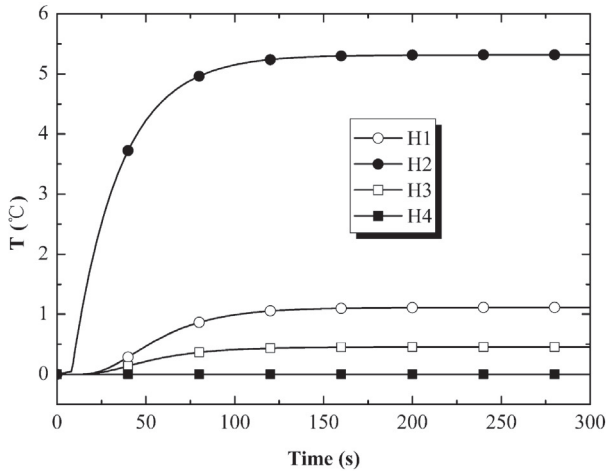
(a) Outlet temperature responses of hot fluids
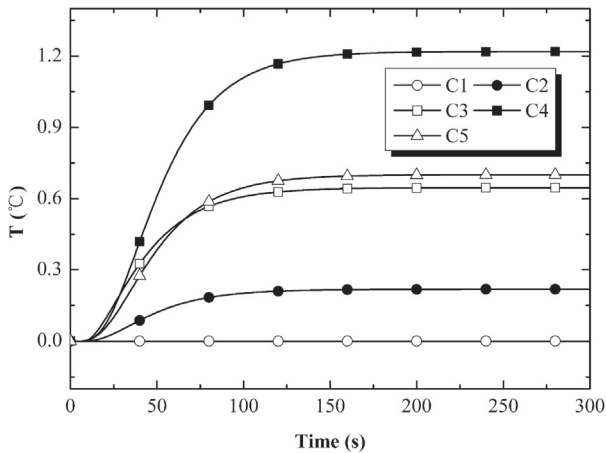
(b) Outlet temperature responses of cold fluids

Fig. 11. Case 4 of transient process under multi disturbances.

be used to investigate the dynamic behavior of HEN with complicated disturbances.

For the forth case of multi-disturbance, the inlet temperature disturbance of 10 K (from 493 K to 503 K) and the mass flow rate disturbance from 2 kg/s to 2.04 kg/s with the percentage of for hot stream H2 are given at some time. The transient responses of the outlet temperature under temperature and flow rate disturbances are shown in Fig. 11. The same tendencies of the temperature responses as Fig. 6 is observed from Fig. 11. Therefore, the availability of the developed method is not relevant to the location of the disturbance.

4. Conclusions

In this paper, signal flow graphs are used to analyze the dynamic behavior and to establish an analytical solution to the dynamic behavior of HEN as follows:

(1) The signal flow graph of the HEN is established according to the transitive relation among streams where a single heat exchanger is treated as a 4×4 MIMO system.
(2) The dynamic input-output relation of the HEN is turned into a signal flow graph, including all of the transfer relationships of the temperature and flow rate in the networks.

(3) Three methods are proposed to obtain the outputs of the whole network, including the outlet nodes and the intermediate nodes in the Laplace domain.
(4) An analytical solution to the dynamic behavior of HEN is presented with the Laplace inverse transform.

To test the effectiveness of the proposed method, a 4×5 HEN is taken as an example. Transient processes under a single disturbance and multi-disturbances are obtained. The conditions are in accordance with the practical conditions, and exact results are obtained. The simulation results obtained illustrated the advantages of the method, including high computation speed, high static and dynamic accuracy, and good adaptability for on-line control and optimal design of the networks.

Acknowledgements

Conflict of interest statement

We declare that we have no financial and personal relationships with other people or organizations that can inappropriately influence our work, there is no professional or other personal interest of any nature or kind in any product, service and/or company that could be construed as influencing the position presented in, or the review of, the manuscript entitled, "An analytical solution to the dynamic behavior of heat exchanger networks".

Appendix A. The expressions of parameters K, T and τ

The gain K

$$K_{ctc} = \frac{\Delta t_{co}}{\Delta t_{ci}} = \frac{\frac{G_c Cp_c}{G_h Cp_h} - 1}{\frac{G_c Cp_c}{G_h Cp_h} - B_c}$$

$$K_{cth} = \frac{\Delta t_{co}}{\Delta t_{hi}} = \frac{1 - B_c}{\frac{G_c Cp_c}{G_h Cp_h} - B_c}$$

$$K_{hth} = \frac{\Delta t_{ho}}{\Delta t_{hi}} = \frac{B_h - B_h \frac{G_h Cp_h}{G_c Cp_c}}{1 - B_h \frac{G_h Cp_h}{G_c Cp_c}}$$

$$K_{htc} = \frac{\Delta t_{ho}}{\Delta t_{ci}} = \frac{1 - B_h}{1 - B_h \frac{G_h Cp_h}{G_c Cp_c}}$$

$$K_{cGc} = \frac{dt_{co}}{dG_c} = \frac{t_{hi} - t_{ci}}{\left(B_c - \frac{G_c Cp_c}{G_h Cp_h}\right)^2}\left(B_c \frac{kA}{G_c G_h Cp_h} + B_c \frac{Cp_c}{G_h Cp_h} - B_c \frac{kA}{G_c^2 Cp_h} - \frac{Cp_c}{G_h Cp_h}\right)$$

$$K_{cGh} = \frac{dt_{co}}{dG_h} = \frac{t_{hi} - t_{ci}}{\left(B_c - \frac{G_c Cp_c}{G_h Cp_h}\right)^2}\left(B_c \frac{k_c A_c}{G_h^2 Cp_h} + \frac{G_c Cp_c}{G_h^2 Cp_h} - B_c \frac{k_c A_c G_c Cp_c}{G_h^3 Cp_h^2} - B_c \frac{G_c Cp_c}{G_h^2 Cp_h}\right)$$

$$K_{hGh} = \frac{dt_{ho}}{dG_h} = \frac{t_{hi} - t_{ci}}{\left(B_h \frac{G_h Cp_h}{G_c Cp_c} - 1\right)^2}\left(B_h \frac{k_h A_h}{G_c^2 Cp_h} + B_h^2 \frac{Cp_h}{G_c Cp_c} - B_h \frac{k_h A_h}{G_h G_c Cp_c} - B_h \frac{Cp_h}{G_c Cp_c}\right)$$

$$K_{hGc} = \frac{dt_{ho}}{dG_c} = \frac{t_{hi} - t_{ci}}{\left(B_h \frac{G_h Cp_h}{G_c Cp_c} - 1\right)^2}\left(B_h \frac{k_h A_h G_h Cp_h}{G_c^2 Cp_c^2} + B_h \frac{G_h Cp_h}{G_c^2 Cp_c} - \frac{k_h A_h}{G_c^2 Cp_c} - B_h^2 \frac{G_h Cp_h}{G_c^2 Cp_c}\right)$$

Note:

K_{ctc}, K_{cth} - the gain of clod fluid out temperature change to cold fluid or hot fluid inlet temperature change.

K_{hth}, K_{htc} - the gains of hot fluid outlet temperature change to hot fluid or cold fluid inlet temperature change.

K_{cGc}, K_{cGh} - the gains of cold fluid outlet temperature change to variation in discharge of cold fluid or hot fluid.

K_{hGh}, K_{hGc} - the gains of hot fluid outlet temperature change to variation in discharge of cold fluid or hot fluid.

where

$$B_c = \frac{t_{hi} - \frac{G_c Cp_c}{G_h Cp_h}(t_{co} - t_{ci}) - t_{ci}}{t_{hi} - t_{co}} \tag{A1}$$

$$B_h = e^{k_h A_h \frac{\frac{G_h Cp_h}{G_c Cp_c} - 1}{\frac{G_c Cp_c}{G_h Cp_h}}} \tag{A2}$$

The time constant T

$$T \qquad = \frac{M_w C_w}{\frac{Cp_c \alpha_c A_c}{Cp_c + \frac{\alpha_c A_c}{2G_c}} + \frac{\alpha_h A_h G_h}{G_h + \frac{\alpha_h A_h}{2Cp_h}}}$$

The delay time τ.

$$\tau \qquad = \begin{cases} 0, & \text{response to flowrate change} \\ \frac{L}{v_{\max}}, & \text{response to inlet temperature change}^* \\ \frac{L}{v_a}, & \text{response to inlet temperature change}^* \end{cases}$$

*In concurrent flow heat exchanger.
**In countercurrent flow heat exchanger.

Appendix B. The Laplace-domain outputs between outlet nodes and source nodes

$Y_{tc1}(s) =$
$W_{cGh1}(s) \times U_{Gh1}(s) + W_{cth1}(s) \times U_{th1}(s)$
$+ W_{cth3}(s) \times W_{ctc1}(s) \times U_{Gh3}(s) + W_{cth3}(s) \times W_{ctc1}(s) \times U_{th3}(s)$
$+ [W_{cGc1}(s) + W_{cGc3}(s) \times W_{ctc1}(s)] \times U_{Gc3}(s) + W_{ctc3}(s) \times W_{ctc1}(s) \times U_{tc3}(s)$

$Y_{tc2}(s) =$
$W_{cth2}(s) \times U_{Gh1}(s) + W_{hth1}(s) \times W_{cth2}(s) \times U_{th1}(s)$
$+ [W_{hth3}(s) \times W_{cth4}(s) \times W_{ctc2}(s) + W_{cth3}(s) \times W_{htc1}(s) \times W_{cth2}(s) + W_{cth4}(s) \times W_{ctc2}(s)] \times U_{Gh3}(s)$
$+ [W_{hth3}(s) \times W_{cth4}(s) \times W_{ctc2}(s) + W_{cth3}(s) \times W_{htc1}(s) \times W_{cth2}(s)] \times U_{th3}(s)$
$+ [W_{hGc3}(s) \times W_{cth4}(s) \times W_{ctc2}(s) + W_{hGc1}(s) \times W_{cth2}(s) + W_{cGc3}(s) \times W_{htc1}(s) \times W_{cth2}(s)] \times U_{Gc3}(s)$
$+ [W_{htc3}(s) \times W_{cth4}(s) \times W_{ctc2}(s) + W_{ctc3}(s) \times W_{htc1}(s) \times W_{cth2}(s)] \times U_{tc3}(s)$
$+ [W_{cGc2}(s) + W_{cGc4}(s) \times W_{ctc2}(s)] \times U_{Gc4}(s) + W_{ctc4}(s) \times W_{ctc2}(s) \times U_{tc4}(s)$

$Y_{th2}(s) =$
$[W_{hth1}(s) \times W_{hth2}(s) + W_{hth2}(s)] \times U_{Gh1}(s) + W_{hth1}(s) \times W_{hth2}(s) \times U_{th1}(s)$
$+ [W_{hth3}(s) \times W_{cth4}(s) \times W_{htc2}(s) + W_{cth3}(s) \times W_{htc1}(s) \times W_{hth2}(s) + W_{cth4}(s) \times W_{htc2}(s)] \times U_{Gh3}(s)$
$+ [W_{hth3}(s) \times W_{cth4}(s) \times W_{htc2}(s) + W_{cth3}(s) \times W_{htc1}(s) \times W_{hth2}(s)] \times U_{th3}(s)$
$+ [W_{hGc3}(s) \times W_{cth4}(s) \times W_{htc2}(s) + W_{hGc1}(s) \times W_{hth2}(s) + W_{cGc3}(s) \times W_{hth2}(s) \times W_{htc1}(s)] \times U_{Gc3}(s)$
$+ [W_{htc3}(s) \times W_{cth4}(s) \times W_{htc2}(s) + W_{ctc3}(s) \times W_{htc1}(s) \times W_{hth2}(s)] \times U_{tc3}(s)$
$+ [W_{hGc2}(s) + W_{cGc4}(s) \times W_{htc2}(s)] \times U_{Gc4}(s) + W_{ctc4}(s) \times W_{htc2}(s) \times U_{tc4}(s)$

$Y_{th4}(s) =$
$[W_{hth3}(s) \times W_{hth4}(s) + W_{hth4}(s)] \times U_{Gh3}(s) + W_{hth3}(s) \times W_{hth4}(s) \times U_{th3}(s)$
$+ W_{hGc3}(s) \times W_{hth4}(s) \times U_{Gc3}(s) + W_{htc3}(s) \times W_{hth4}(s) \times U_{tc3}(s)$
$+ W_{hGc4}(s) \times U_{Gc4}(s) + W_{htc4}(s) \times U_{tc4}(s)$

Appendix C. The total output of the signal flow graph of $Y_{th4}(s)$

$Y_{th4}(s)$
$= W_{hth4}(s) \times U_{th4}(s) + W_{hth4}(s) \times U_{Gh4}(s) + W_{hGc4}(s) \times U_{Gc4}(s) + W_{htc4}(s) \times U_{tc4}(s)$
$= W_{hGc4}(s) \times U_{Gc4}(s) + W_{htc4}(s) \times U_{tc4}(s) + W_{hth4}(s) \times U_{Gh3}(s)$
$+ W_{hth4}(s) \times [W_{htc3}(s) \times U_{tc3}(s) + W_{hGc3}(s) \times U_{Gc3}(s) + W_{hth3}(s) \times U_{th3}(s) + W_{hth3}(s) \times U_{Gh3}(s)]$
$= W_{hGc4}(s) \times U_{Gc4}(s) + W_{htc4}(s) \times U_{tc4}(s)$
$+ W_{hGc3}(s) \times W_{hth4}(s) \times U_{Gc3}(s) + W_{htc3}(s) \times W_{hth4}(s) \times U_{tc3}(s)$
$+ [W_{hth3}(s) \times W_{hth4}(s) + W_{hth4}(s)] \times U_{Gh3}(s) + W_{hth3}(s) \times W_{hth4}(s) \times U_{th3}(s)$

Appendix D. The Laplace domain outputs of the outlet temperatures

$Y_{th8}(s) =$
$U_{Gc1}(s) \times [W_{hGc1}(s)W_{cth4}(s)W_{htc5}(s)W_{hth8}(s) + W_{hGc3}(s)W_{hth5}(s)W_{hth8}(s)$
$+ W_{cGc2}(s)W_{htc3}(s)W_{hth5}(s)W_{hth8}(s) + W_{cGc1}(s)W_{ctc2}(s)W_{htc3}(s)W_{hth5}(s)W_{hth8}(s)]$
$+ U_{tc1}(s)[W_{htc1}(s)W_{cth4}(s)W_{htc5}(s)W_{hth8}(s) + W_{ctc1}(s)W_{ctc2}(s)W_{htc3}(s)W_{hth5}(s)W_{hth8}(s)]$
$+ U_{th1}(s)[W_{hth1}(s)W_{cth4}(s)W_{htc5}(s)W_{hth8}(s) + W_{cth1}(s)W_{ctc2}(s)W_{htc3}(s)W_{hth5}(s)W_{hth8}(s)]$
$+ U_{Gh1}(s)[W_{hGh1}(s)W_{cth4}(s)W_{htc5}(s)W_{hth8}(s) + W_{cGh4}(s)W_{htc5}(s)W_{hth8}(s)$
$+ W_{cGh1}(s)W_{ctc2}(s)W_{htc3}(s)W_{hth5}(s)W_{hth8}(s)]$
$+ U_{th2}(s)W_{cth2}(s)W_{htc3}(s)W_{hth5}(s)W_{hth8}(s) + U_{Gh2}(s)W_{cGh2}(s)W_{htc3}(s)W_{hth5}(s)W_{hth8}(s)$
$+ U_{th3}(s)W_{hth3}(s)W_{hth5}(s)W_{hth8}(s)$
$+ U_{Gh3}(s)[W_{hGhs}(s)W_{hth8}(s) + W_{hGh3}(s)W_{hth5}(s)W_{hth8}(s) + W_{hGh8}(s)]$
$+ U_{Gc4}(s)[W_{hGc5}(s)W_{hth8}(s) + W_{cGc4}(s)W_{htc5}(s)W_{hth8}(s)]$
$+ U_{tc4}(s)W_{ctc4}(s)W_{htc5}(s)W_{hth8}(s) + U_{Gc8}(s)W_{hGc8}(s) + U_{tc8}(s)W_{htc8}(s)$

$Y_{th2}(s) =$

$$
\begin{aligned}
Y_{th9}(s) = \quad & U_{Gc1}(s)[W_{hGc2}(s) + W_{cGc1}(s)W_{htc2}(s)] + U_{tc1}(s)W_{ctc1}(s)W_{htc2}(s) \\
& + U_{th1}(s)W_{cth1}(s)W_{htc2}(s) + U_{Gh1}(s)W_{cGh1}(s)W_{htc2}(s) \\
& + U_{th2}(s)W_{hth2}(s) + U_{Gh2}(s)W_{hGh2}(s) \\
\end{aligned}
$$

$$
\begin{aligned}
Y_{th9}(s) = \quad & U_{Gc1}(s)[W_{hGc1}(s)W_{cth4}(s)W_{ctc5}(s)W_{htc6}(s)W_{hth9}(s) \\
& + W_{hGc3}(s)W_{cth5}(s)W_{htc6}(s)W_{hth9}(s) + W_{cGc2}(s)W_{htc3}(s)W_{cth5}(s)W_{htc6}(s)W_{hth9}(s) \\
& + W_{ctc1}(s)W_{ctc2}(s)W_{htc3}(s)W_{cth5}(s)W_{htc6}(s)W_{hth9}(s)] \\
& + U_{tc1}(s)[W_{htc1}(s)W_{cth4}(s)W_{ctc5}(s)W_{htc6}(s)W_{hth9}(s) \\
& + W_{ctc1}(s)W_{ctc2}(s)W_{htc3}(s)W_{cth5}(s)W_{htc6}(s)W_{hth9}(s)] \\
& + U_{th1}(s)[W_{htc1}(s)W_{cth4}(s)W_{ctc5}(s)W_{htc6}(s)W_{hth9}(s) \\
& + W_{ctc1}(s)W_{ctc2}(s)W_{htc3}(s)W_{cth5}(s)W_{htc6}(s)W_{hth9}(s)] \\
& + U_{Gh1}(s)[W_{hGh1}(s)W_{cth4}(s)W_{ctc5}(s)W_{htc6}(s)W_{hth9}(s) \\
& + W_{cGh4}(s)W_{ctc5}(s)W_{htc6}(s)W_{hth9}(s) + W_{cGh1}(s)W_{ctc2}(s)W_{htc3}(s)W_{cth5}(s)W_{htc6}(s)W_{hth9}(s)] \\
& + U_{th2}(s)W_{cth2}(s)W_{htc3}(s)W_{cth5}(s)W_{htc6}(s)W_{hth9}(s) \\
& + U_{Gh2}(s)W_{htc3}(s)W_{cth5}(s)W_{htc6}(s)W_{hth9}(s) + U_{th3}(s)W_{hth3}(s)W_{cth5}(s)W_{htc6}(s)W_{hth9}(s) \\
& + U_{Gh3}(s)[W_{hGh3}(s)W_{cth5}(s)W_{htc6}(s)W_{hth9}(s) + W_{cGh5}(s)W_{htc6}(s)W_{hth9}(s)] \\
& + U_{Gc4}(s)[W_{cGc5}(s)W_{htc6}(s)W_{hth9}(s) \\
& + W_{cGc4}(s)W_{ctc5}(s)W_{htc6}(s)W_{hth9}(s) + W_{hGc6}(s)W_{hth9}(s)] \\
& + U_{tc4}(s)W_{ctc4}(s)W_{ctc5}(s)W_{htc6}(s)W_{hth9}(s) + U_{th6}(s)W_{hth6}(s)W_{hth9}(s) \\
& + U_{Gh6}(s)[W_{hGh6}(s)W_{hth9}(s) + W_{hGh9}(s)] + U_{Gc9}(s)W_{hGc9}(s) + U_{tc9}(s)W_{htc9}(s) \\
\end{aligned}
$$

$$
\begin{aligned}
Y_{th7}(s) = \quad & U_{Gh1}(s) \times [W_{hGh7}(s) + W_{hGh1}(s)W_{hth4}(s)W_{hth7}(s) + W_{hGh4}(s)W_{hth7}(s)] \\
& + U_{Gc1}(s) \times W_{hGc1}(s)W_{hth4}(s)W_{hth7}(s) + U_{tc1}(s) \times W_{htc1}(s)W_{hth4}(s)W_{hth7}(s) \\
& + U_{th1}(s) \times W_{hth1}(s)W_{hth4}(s)W_{hth7}(s) + U_{tc4}(s) \times W_{htc4}(s)W_{hth7}(s) \\
& + U_{Gc4}(s) \times W_{hGc4}(s)W_{hth7}(s) + U_{Gc7}(s) \times W_{hGc7}(s) + U_{tc7}(s) \times W_{htc7}(s) \\
\end{aligned}
$$

$$
\begin{aligned}
Y_{tc7}(s) = \quad & U_{Gc7}(s)W_{cGc7}(s) + U_{tc7}(s)W_{ctc7}(s) \\
& + U_{Gh1}(s)[W_{cGh7}(s) + W_{hGh1}(s)W_{hth4}(s)W_{cth7}(s) + W_{hGh4}(s)W_{cth7}(s)] \\
& + U_{Gc4}(s)W_{hGc4}(s)W_{cth7}(s) + U_{tc4}(s)W_{htc4}(s)W_{cth7}(s) \\
& + U_{Gc1}(s)W_{hGc1}(s)W_{hth4}(s)W_{cth7}(s) + U_{tc1}(s)W_{htc1}(s)W_{hth4}(s)W_{cth7}(s) \\
& + U_{th1}(s)W_{hth1}(s)W_{hth4}(s)W_{cth7}(s) \\
\end{aligned}
$$

$$
\begin{aligned}
Y_{tc6}(s) = \quad & U_{Gh1}(s)[W_{cGh4}(s)W_{ctc5}(s)W_{ctc6}(s) + W_{hGh1}(s)W_{cth4}(s)W_{ctc5}(s)W_{ctc6}(s) \\
& + W_{cGh1}(s)W_{ctc2}(s)W_{htc3}(s)W_{cth5}(s)W_{ctc6}(s)] \\
& + U_{Gc1}(s)[W_{hGc1}(s)W_{cth4}(s)W_{ctc5}(s)W_{ctc6}(s) + W_{hGc3}(s)W_{cth5}(s)W_{ctc6}(s) \\
& + W_{cGc2}(s)W_{htc3}(s)W_{cth5}(s)W_{ctc6}(s) + W_{cGc1}(s)W_{ctc2}(s)W_{htc3}(s)W_{cth5}(s)W_{ctc6}(s)] \\
& + U_{tc1}(s)[W_{htc1}(s)W_{cth4}(s)W_{ctc5}(s)W_{ctc6}(s) + W_{ctc1}(s)W_{ctc2}(s)W_{htc3}(s)W_{cth5}(s)W_{ctc6}(s)] \\
& + U_{th1}(s)[W_{hth1}(s)W_{cth4}(s)W_{ctc5}(s)W_{ctc6}(s) + W_{ctc1}(s)W_{ctc2}(s)W_{htc3}(s)W_{cth5}(s)W_{ctc6}(s)] \\
& + U_{th2}(s)W_{cth2}(s)W_{htc3}(s)W_{cth5}(s)W_{ctc6}(s) + U_{Gh2}(s)W_{cGh2}(s)W_{htc3}(s)W_{cth5}(s)W_{ctc6}(s) \\
& + U_{th3}(s)W_{hth3}(s)W_{cth5}(s)W_{ctc6}(s) \\
& + U_{Gh3}(s)[W_{cGh5}(s)W_{ctc6}(s) + W_{hGh3}(s)W_{cth5}(s)W_{ctc6}(s)] \\
& + U_{Gc4}(s)[W_{cGc6}(s) + W_{cGc5}(s)W_{ctc6}(s) + W_{cGc4}(s)W_{ctc5}(s)W_{ctc6}(s)] \\
& + U_{tc4}(s)W_{ctc4}(s)W_{ctc5}(s)W_{ctc6}(s) + U_{th6}(s)W_{cth6}(s) + U_{Gh6}(s)W_{cGh6}(s) \\
\end{aligned}
$$

$$
\begin{aligned}
Y_{tc3}(s) = \quad & U_{Gc1}(s)[W_{cGc3}(s) + W_{cGc2}(s)W_{ctc3}(s) + W_{cGc1}(s)W_{ctc2}(s)W_{ctc3}(s)] \\
& + U_{Gh1}(s)W_{cGh1}(s)W_{ctc2}(s)W_{ctc3}(s) + U_{tc1}(s)W_{ctc1}(s)W_{ctc2}(s)W_{ctc3}(s) \\
& + U_{th1}(s)W_{cth1}(s)W_{ctc2}(s)W_{ctc3}(s) + U_{th2}(s)W_{cth2}(s)W_{ctc3}(s) \\
& + U_{Gh2}(s)W_{cGh2}(s)W_{ctc3}(s) + U_{th3}(s)W_{cth3}(s) + U_{Gh3}(s)W_{cGh3}(s) \\
\end{aligned}
$$

$$
\begin{aligned}
Y_{tc8}(s) = \quad & U_{Gc1}(s)[W_{hGc1}(s)W_{cth4}(s)W_{htc5}(s)W_{cth8}(s) + W_{hGc3}(s)W_{hth5}(s)W_{cth8}(s) \\
& + W_{cGc2}(s)W_{htc3}(s)W_{hth5}(s)W_{cth8}(s) + W_{cGc1}(s)W_{ctc2}(s)W_{htc3}(s)W_{hth5}(s)W_{cth8}(s)] \\
& + U_{tc1}(s)[W_{htc1}(s)W_{cth4}(s)W_{htc5}(s)W_{cth8}(s) \\
& + W_{ctc1}(s)W_{ctc2}(s)W_{htc3}(s)W_{hth5}(s)W_{cth8}(s)] \\
& + U_{th1}(s)[W_{hth1}(s)W_{cth4}(s)W_{htc5}(s)W_{cth8}(s) \\
& + W_{ctc1}(s)W_{ctc2}(s)W_{htc3}(s)W_{hth5}(s)W_{cth8}(s)] \\
& + U_{Gh1}(s)[W_{hGh1}(s)W_{cth4}(s)W_{htc5}(s)W_{cth8}(s) + W_{cGh4}(s)W_{htc5}(s)W_{cth8}(s) \\
& + W_{cGh1}(s)W_{ctc2}(s)W_{htc3}(s)W_{hth5}(s)W_{cth8}(s)] \\
& + U_{th2}(s)W_{cth2}(s)W_{htc3}(s)W_{hth5}(s)W_{cth8}(s) \\
& + U_{Gh2}(s)W_{cGh2}(s)W_{htc3}(s)W_{hth5}(s)W_{cth8}(s) \\
& + U_{th3}(s)W_{hth3}(s)W_{hth5}(s)W_{cth8}(s) \\
& + U_{Gh3}(s)[W_{hGh5}(s)W_{cth8}(s) + W_{hGh3}(s)W_{hth5}(s)W_{cth8}(s) + W_{cGh8}(s)] \\
& + U_{Gc4}(s)[W_{hGc5}(s)W_{cth8}(s) + W_{cGc4}(s)W_{htc5}(s)W_{cth8}(s)] \\
& + U_{tc4}(s)W_{htc5}(s)W_{cth8}(s) + U_{Gc8}(s)W_{cGc8}(s) + U_{tc8}(s)W_{ctc8}(s) \\
\end{aligned}
$$

$$
\begin{aligned}
Y_{tc9}(s) = \ & U_{Gc1}(s)[W_{hGc1}(s)W_{cth4}(s)W_{ctc5}(s)W_{htc6}(s)W_{cth9}(s) \\
& + W_{hGc3}(s)W_{cth5}(s)W_{htc6}(s)W_{cth9}(s) + W_{cGc2}(s)W_{htc3}(s)W_{cth5}(s)W_{htc6}(s)W_{cth9}(s) \\
& + W_{cGc1}(s)W_{ctc2}(s)W_{htc3}(s)W_{cth5}(s)W_{htc6}(s)W_{cth9}(s)] \\
& + U_{tc1}(s)[W_{htc1}(s)W_{cth4}(s)W_{ctc5}(s)W_{htc6}(s)W_{cth9}(s) \\
& + W_{ctc1}(s)W_{ctc2}(s)W_{htc3}(s)W_{cth5}(s)W_{htc6}(s)W_{cth9}(s)] \\
& + U_{th1}(s)[W_{th1}(s)W_{cth4}(s)W_{ctc5}(s)W_{htc6}(s)W_{cth9}(s) \\
& + W_{cth1}(s)W_{ctc2}(s)W_{htc3}(s)W_{cth5}(s)W_{htc6}(s)W_{cth9}(s)] \\
& + U_{Gh1}(s)[W_{hGh1}(s)W_{cth4}(s)W_{ctc5}(s)W_{htc6}(s)W_{cth9}(s) \\
& + W_{cGh4}(s)W_{ctc5}(s)W_{htc6}(s)W_{cth9}(s) \\
& + W_{cGh1}(s)W_{ctc2}(s)W_{htc3}(s)W_{cth5}(s)W_{htc6}(s)W_{cth9}(s)] \\
& + U_{th2}(s)W_{cth2}(s)W_{htc3}(s)W_{cth5}(s)W_{htc6}(s)W_{cth9}(s) \\
& + U_{Gh2}(s)W_{cGh2}(s)W_{htc3}(s)W_{cth5}(s)W_{htc6}(s)W_{cth9}(s) \\
& + U_{th3}(s)W_{hth3}(s)W_{cth5}(s)W_{htc6}(s)W_{cth9}(s) \\
& + U_{Gh3}(s)[W_{hGh3}(s)W_{cth5}(s)W_{htc6}(s)W_{cth9}(s) + W_{cGh5}(s)W_{htc6}(s)W_{cth9}(s)] \\
& + U_{Gc4}(s)[W_{cGc5}(s)W_{htc6}(s)W_{cth9}(s) + W_{cGc4}(s)W_{ctc5}(s)W_{htc6}(s)W_{cth9}(s) + W_{hGc6}(s)W_{cth9}(s)] \\
& + U_{tc4}(s)W_{ctc4}(s)W_{ctc5}(s)W_{htc6}(s)W_{cth9}(s) + U_{th6}(s)W_{hth6}(s)W_{cth9}(s) \\
& + U_{Gh6}(s)[W_{hGh6}(s)W_{cth9}(s) + W_{cGh9}(s)] \\
& + U_{Gc9}(s)W_{cGc9}(s) + U_{tc9}(s)W_{ctc9}(s)
\end{aligned}
$$

Appendix E. The time-domain output responses of the HEN

$$
\begin{aligned}
Y_{th8}(s) = \ & \begin{bmatrix} 3.5741 \times \exp(-0.7927 \times 10^{-1} \times t + 1.2954) - \\ 3.5604 \times \exp(-1.1944 \times 10^{-1} \times t + 1.9520) - \\ 39.6107 \times \exp(-1.7579 \times 10^{-1} \times t + 2.8728) - \\ 1.7996 \times \exp(-0.3773 \times 10^{-1} \times t + 0.6166) + \\ 40.999 \times \exp(-1.7495 \times 10^{-1} \times t + 2.8592) + 0.3974 \end{bmatrix} \times H(t - 16.3423) \\
& + \begin{bmatrix} 5015.8010 \times \exp(-1.7579 \times 10^{-1} \times t + 1.6730) - \\ 5419.8299 \times \exp(-1.7495 \times 10^{-1} \times t + 1.6650) - \\ 39.8438 \times \exp(-1.1944 \times 10^{-1} \times t + 1.1367) + \\ 442.8284 \times \exp(-1.6901 \times 10^{-1} \times t + 1.5314) + 1.0443 \end{bmatrix} \times H(t - 9.5169)
\end{aligned}
$$

$$
Y_{th2}(s) = 4.1976 + 4.1976 \times \exp(-1.0676 \times 10^{-1} \times t) \times \begin{bmatrix} -\cosh(0.6903 \times 10^{-1} \times t) \\ -1.5465 \times \sinh(0.6903 \times 10^{-1} \times t) \end{bmatrix}
$$

$$
\begin{aligned}
Y_{th9}(s) = \ & \begin{bmatrix} 126.4833 \times \exp(-1.7579 \times 10^{-1} \times t + 2.2858) - \\ 125.2047 \times \exp(-1.7495 \times 10^{-1} \times t + 2.2750) + \\ 0.4748 \times \exp(-2.5192 \times 10^{-1} \times t + 3.2757) + \\ 1.1248 \times \exp(-0.7927 \times 10^{-1} \times t + 1.0307) - \\ 0.7168 \times \exp(-0.3773 \times 10^{-1} \times t + 0.4906) - \\ 2.3244 \times \exp(-2.1987 \times 10^{-1} \times t + 2.892) + 0.1629 \end{bmatrix} \times H(t - 13.0031) \\
& + \begin{bmatrix} 4534.2170 \times \exp(-1.7579 \times 10^{-1} \times t + 2.2888) - \\ 184.2623 \times \exp(-2.5192 \times 10^{-1} \times t + 3.2799) + \\ 4685.6707 \times \exp(-1.7495 \times 10^{-1} \times t + 2.2779) - \\ 7.7217 \times \exp(-0.8280 \times 10^{-1} \times t + 3.2342) + \\ 40.4091 \times \exp(-2.1987 \times 10^{-1} \times t + 2.8627) + 0.1212 \end{bmatrix} \times H(t - 13.0198)
\end{aligned}
$$

$$
Y_{th7}(s) = \begin{bmatrix} 5.9275 \times \exp(-1.6091 \times 10^{-1} \times t + 2.0382) - \\ 3.2919 \times \exp(-0.2945 \times 10^{-1} \times t + 0.3731) - \\ 4.8742 \times \exp(-1.7579 \times 10^{-1} \times t + 2.2267) + 2.2386 \end{bmatrix} \times H(t - 12.6666)
$$

$$
Y_{tc7}(s) = \begin{bmatrix} 3.074 \times \exp(-1.6091 \times 10^{-1} \times t + 1.6091) - \\ 1.7074 \times \exp(-0.2945 \times 10^{-1} \times t + 0.2945) - \\ 2.5280 \times \exp(-1.7579 \times 10^{-1} \times t + 1.7579) + 1.1611 \end{bmatrix} \times H(t - 10.)
$$

$Y_{tc6}(s) =$

$$Y_{tc3}(s) = \begin{bmatrix} 18.3049 \times \exp(-1.7579 \times 10^{-1} \times t + 2.0262) - \\ 18.3187 \times \exp(-1.7495 \times 10^{-1} \times t + 2.0166) - \\ 0.2918 \times \exp(-0.3773 \times 10^{-1} \times t + 0.4348) + \\ 0.3691 \times \exp(-0.7927 \times 10^{-1} \times t + 0.9137) - \\ 0.1416 \times \exp(-2.1987 \times 10^{-1} \times t + 2.5343) + 0.0780 \end{bmatrix} \times H(t - 11.5262)$$

$$+ \begin{bmatrix} 685.5609 \times \exp(-1.7495 \times 10^{-1} \times t + 2.0195) - \\ 31.8784 \times \exp(-1.6091 \times 10^{-1} \times t + 1.8574) + \\ 2.4617 \times \exp(-2.1987 \times 10^{-1} \times t + 2.5380) - \\ 656.2022 \times \exp(-1.7579 \times 10^{-1} \times t + 2.0291) + 0.0580 \end{bmatrix} \times H(t - 11.5429)$$

$$Y_{tc8}(s) = \begin{bmatrix} 0.3821 \times \exp(-0.7927 \times 10^{-1} \times t + 1.2508) - \\ 0.0518 \times \exp(-1.7579 \times 10^{-1} \times t + 2.7739) - \\ 0.5613 \times \exp(-0.3773 \times 10^{-1} \times t + 0.5953) + 0.2310 \end{bmatrix} \times H(t - 15.7796)$$

$$\begin{bmatrix} 44.9855 \times \exp(-1.7495 \times 10^{-1} \times t + 1.9717) - \\ 3.9066 \times \exp(-1.1944 \times 10^{-1} \times t + 1.3461) - \\ 43.4619 \times \exp(-1.7579 \times 10^{-1} \times t + 1.9811) + \\ 1.9746 \times \exp(-0.3773 \times 10^{-1} \times t + 0.4252) - \\ 3.9216 \times \exp(-0.7927 \times 10^{-1} \times t + 0.8933) + 0.4360 \end{bmatrix} \times H(t - 11.2698)$$

$$+ \begin{bmatrix} 5503.4718 \times \exp(-1.7579 \times 10^{-1} \times t + 2.0195) - \\ 5946.7832 \times \exp(-1.7579 \times 10^{-1} \times t + 0.7775) + \\ 43.7177 \times \exp(-1.1944 \times 10^{-1} \times t + 0.5308) - \\ 485.8833 \times \exp(-1.6091 \times 10^{-1} \times t + 0.7151) + 1.1458 \end{bmatrix} \times H(t - 4.4444)$$

$$Y_{tc9}(s) = \begin{bmatrix} 194.4157 \times \exp(-1.7579 \times 10^{-1} \times t + 1.3951) - \\ 192.4503 \times \exp(-1.7579 \times 10^{-1} \times t + 1.3885) - \\ 0.7298 \times \exp(-2.5192 \times 10^{-1} \times t + 1.9993) + \\ 1.7289 \times \exp(-0.7927 \times 10^{-1} \times t + 0.6291) - \\ 1.1017 \times \exp(-0.3773 \times 10^{-1} \times t + 0.2994) - \\ 3.5728 \times \exp(-2.1987 \times 10^{-1} \times t + 1.7450) + 0.2505 \end{bmatrix} \times H(t - 7.9365)$$

$$+ \begin{bmatrix} 62.1122 \times \exp(-2.1987 \times 10^{-1} \times t + 1.7487) - \\ 6969.4776 \times \exp(-1.7579 \times 10^{-1} \times t + 1.3981) + \\ 283.2269 \times \exp(-1.6091 \times 10^{-1} \times t + 1.2798) - \\ 7202.2749 \times \exp(-1.7579 \times 10^{-1} \times t + 1.3914) - \\ 11.8690 \times \exp(-2.5192 \times 10^{-1} \times t + 2.0035) + 0.1863 \end{bmatrix} \times H(t - 7.9532)$$

Note: $H(t)$ is the Heaviside function, where

$$H(t) = \begin{cases} 0, & t < 0 \\ 1, & t \geqslant 0 \end{cases} \tag{E1}$$

Appendix F. Supplementary material

Supplementary data associated with this article can be found, in the online version, at https://doi.org/10.1016/j.ijheatmasstransfer. 2018.05.041.

References

[1] S.K. Das, T.K. Dan, Transient response of a parallel flow shell-and-tube heat exchanger and its control, Heat Mass Transf. 31 (4) (1996) 231–235.

[2] F. Bagui, H. Chafouk, Transient heat transfert in coflow heat exchanger, Heat Mass Transf. 42 (9) (2006) 835–841.

[3] K. Zheng, H.H. Lou, J. Wang, et al., A method for flexible heat exchanger network design under severe operation uncertainty, Chem. Eng. Technol. 36 (5) (2013) 757–765.

[4] S.M. Shahril, G.A. Quadir, N.A.M. Amin, et al., Numerical investigation on the thermohydraulic performance of a shell-and-double concentric tube heat exchanger using nanofluid under the turbulent flow regime, Numer. Heat Transfer; Part A: Appl. 71 (2) (2017) 215–231.

[5] A.H. Saberi, M. Kalteh, Numerical investigation of nanofluid flow and conjugated heat transfer in a micro-heat-exchanger using the lattice Boltzmann method, Numer. Heat Transfer; Part A: Appl. 70 (12) (2016) 1390–1401.

[6] Y. Wang, Y.L. He, Y.S. Li, et al., Theoretical study of air-side volatility effects on the performance of H-type finned heat exchangers in waste heat utilization, Numer. Heat Transfer; Part A: Appl. 70 (6) (2016) 613–638.

[7] Z. Zhao, D. Che, Y. Zhang, et al., Numerical investigation on conjugate heat transfer to supercritical CO 2 in membrane helical coiled tube heat exchangers, Numer. Heat Transfer; Part A: Appl. 69 (9) (2016) 977–995.

[8] X. Chen, F. Tavakkoli, K. Vafai, Analysis and characterization of metal foam-filled double-pipe heat exchangers, Numer. Heat Transfer; Part A: Appl. 68 (10) (2015) 1031–1049.

[9] M. Ismail, A. Fartaj, M. Karimi, Numerical investigation on heat transfer and fluid flow behaviors of viscous fluids in a minichannel heat exchanger, Numer. Heat Transfer; Part A: Appl. 64 (1) (2013) 1–29.

[10] A.R. Khan, N.S. Baker, A.P. Wardle, The dynamic characteristics of a countercurrent plate heat exchanger, Int. J. Heat Mass Transf. 31 (6) (1988) 1269–1278.

[11] C.C. Lakshmanan, O.E. Potter, Dynamic simulation of plate heat exchangers, Int. J. Heat Mass Transf. 33 (5) (1990) 995–1002.

[12] G.W. Mcknight, C.W. Worley, Dynamic analysis of plate heat exchanger system, in: ISA Proceedings, 1953, pp. 68–75.

[13] W. Roetzel, Y. Xuan, Analysis of transient behaviour of multipass shell and tube heat exchangers with the dispersion model, Int. J. Heat Mass Transf. 35 (1) (1992) 2953–2962.

[14] M.N. Roppo, E.N. Ganl, Time-dependent heat exchanger modeling, Heat Transfer Eng. 4 (2) (1983) 42–46.

[15] J.L. Marchetti, Dynamic simulation of shell-and-tube heat exchangers, Heat Transfer Eng. 8 (1) (1987) 50–59.

[16] W. Roetzel, Y. Xuan, Transient behaviour of multipass shell-and-tube heat exchangers, Int. J. Heat Mass Transf. 35 (3) (1992) 707–710.

[17] F.E. Romie, Transient response of the parallel-flow heat exchanger, J. Heat Transfer 107 (3) (1985) 727–730.

[18] C.H. Li, Exact transient solutions of parallel-current transfer processes, J. Heat Transfer 108 (2) (1986) 365–369.

[19] F.E. Romie, Transient response of the counterflow heat exchanger, J. Heat Transfer 106 (3) (1984) 620–626.

[20] F. Sharifi, M.R.G. Narandji, K. Mehravaran, Dynamic simulation of plate heat exchangers, Int. Commun. Heat Mass Transfer 22 (2) (1995) 213–225.

[21] A.E.S. Konukman, U. Akman, Flexibility and operability analysis of a HEN-integrated natural gas expander plant, Chem. Eng. Sci. 60 (24) (2005) 7057–7074.

[22] K.W. Mathisen, M. Morari, S. Skogestad, Dynamic models for heat exchangers and heat exchanger networks, Comput. Chem. Eng. 18 (1) (1994) S459–S463.

[23] R. Tellez, W.Y. Svrcek, T.J. Ross, et al., Heat exchanger network process modifications for controllability using design reliability theory, Comput. Chem. Eng. 30 (4) (2006) 730–743.

[24] S. Hernández, L. Balcazar-López, J.A. Sánchez-Márquez, et al., Controllability and operability analysis of heat exchanger networks including bypasses, Chem. Biochem. Eng. Q. 24 (1) (2010) 23–28.

[25] E.I. Varga, K.M. Hangos, F. Szigeti, Controllability and observability of heat exchanger networks in the time-varying parameter case, Control Eng. Pract. 3 (3) (2015) 1409–1419.

[26] J.A. Francesconi, D.G. Oliva, P.A. Aguirre, Flexible heat exchanger network design of an ethanol processor for hydrogen production. A model-based multi-objective optimization approach, Int. J. Hydrogen Energy 42 (5) (2016) 2736–2747.

[27] C. Boyaci, D. Uztürk, A.E.Ş. Konukman, et al., Dynamics and optimal control of flexible heat-exchanger networks, Comput. Chem. Eng. 20 (12) (1996) S775–S780.

[28] M. Baldea, P. Daoutidis, Model reduction and control of reactor–heat exchanger networks, J. Process Control 16 (3) (2006) 265–274.

[29] C. Guha, A. Chaudhuri, Transient analysis of heat exchanger network, J. Inst. Engineers Chem. Eng. Division (India) 33 (2007) 51–59.

[30] M. Lachi, N.E. Wakil, J. Padet, The time constant of double pipe and one pass shell-and-tube heat exchangers in the case of varying fluid flow rates, Int. J. Heat Mass Transf. 40 (9) (1997) 2067–2079.

[31] F.E. Romie, Response of counterflow heat exchangers to step changes of flow rates, Trans. Asme Ser. C J. Heat Transfer 121 (3) (1999) 746–748.

[32] W. Roetzel, Y. Xuan, Transient response of parallel and counterflow heat exchangers, J. Heat Transfer 114 (2) (1992) 510–512.

[33] G.M. Cui, J.Y. Wang, T. Jiang, et al., Transfer behavior of heat exchanger, Adv. Mater. Res. 233–235 (2011) 1281–1287.

[34] F.Z aversky, Margaret spellings anchez, da strain, Object - oriented modeling for the transient response simulation of multi - pass shell - and - tube heat exchangers as applied in active in direct thermal energy storage systems for concentrated solar Power, Energy 65 (2014) 647–664.

[35] M. Trafczynski, M. Markowski, S. Alabrudzinski, et al., The influence of fouling on the dynamic behavior of PID-controlled heat exchangers, Appl. Therm. Eng. 109 (2016) 727–738.

[36] T.F. Yee, I.E. Grossmann, Simultaneous optimization models for heat integration II. Heat exchanger network synthesis, Comput. Chem. Eng. 14 (10) (1990) 1165–1184.

[37] S.D. Eppinger, M.V. Nukala, D.E. Whitney, Generalised models of design interation using signal flow graphs, Res. Eng. Des. 9 (2) (1997) 112–123.

[38] S.J. Mason, Feedback theory-some properties of signal flow graphs, Proc. Ire 41 (9) (1956) 1144–1156.

[39] J.X. Chen, G.M. Cui, H.H. Duan, Multipopulation differential evolution algorithm based on the opposition-based learning for heat exchanger network synthesis, Numer. Heat Transfer, Part A: Appl. 72 (2) (2017) 126–140.